

# Parameter Estimation for Subtidal Water Levels Using An Adjoint Variational Optimal Method

Aijun Zhang<sup>1</sup>, Eugene Wei<sup>1</sup>, and Bruce Parker<sup>1</sup>

## Abstract

In this paper, the two-dimensional Princeton Ocean Model (POM) (Blumberg and Mellor, 1987; Mellor, 1998) is implemented to simulate wind-driven subtidal water levels along the U.S. East Coast. The model is forced by a 48km ETA Data Assimilation System (EDAS) analyzed wind field. An optimal adjoint variational data assimilation technique is presented to assimilate the subtidal water levels sampled along the entire Atlantic Coast of the U.S. into the numerical model. In the optimal data assimilation procedure, the subtidal water level misfit is defined as the cost function. The gradient of cost function is determined by the adjoint model. Limited memory Broyden-Fletcher-Goldfarb-Shanno (BFGS) quasi-Newton (Liu and Nocedal, 1989) method for large scale optimization is implemented to minimize the cost function. The data assimilation system was tested in ideal twin identical experimental cases in which the pseudo-observations are generated by numerical model with predefined wind drag coefficients ( $C_d$ ). The results show that the wind drag coefficients can be recovered from subtidal water levels very accurately by using this adjoint optimal data assimilation system.

## 1. Introduction

In recent years, data assimilation techniques based on optimal control methods have been developed and widely applied in meteorologic and oceanographic fields. As early as 1970's, the adjoint approach with the governing equations as strong constraints was described by Sasaki (1970a,b) which gave a framework that is readily

---

<sup>1</sup>Coast Survey Development Laboratory, NOS/NOAA, 1315 East-West Hwy., Silver Spring, MD 20910; E-mail: aijun.zhang@noaa.gov

applicable to a set of steady or unsteady state equations. Yu and O'Brien (1991) used a variational adjoint method in a one-dimensional vertical model to estimate the wind stress drag coefficient and the oceanic eddy viscosity profile from observed velocity data. Schwab (1982) used the inverse method to estimate wind stress from water level fluctuations. Das and Lardner (1991) implemented the adjoint method to

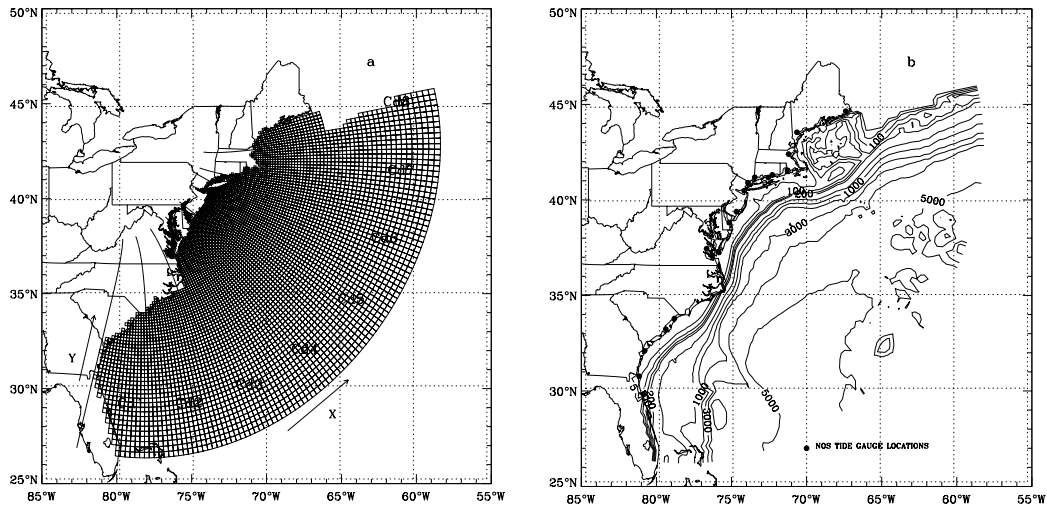


Fig. 1. U.S. East Coast subtidal water level forecast system, (a) computational grid; (b) tide gauge locations and bathymetry.

determine the bottom friction coefficient and water depth which are position dependent parameters from periodic tidal data. Panchang and O'Brien (1989) applied adjoint state formulation to a one-dimensional hydraulic model to determine the bottom friction factor for a tidal river. Chu et al. (1997) determined open boundary conditions with an optimization method, in which a multiperturbation method is proposed to determine the gradient of cost function. Thus, his method is independent of the ocean model and can be easily applied to linear and nonlinear ocean models. But for the case of a large number of control variables, the multiperturbation method for determining the gradient of the cost function is time consuming.

With POM being widely used by more and more oceanographers (Aikman et al 1996; Mellor and Ezer 1991; Ezer and Mellor 1997) and variational adjoint techniques being successfully applied in many fields, it is possible and necessary to develop an adjoint model of POM in order to efficiently perform data assimilation.

For the purpose of water level forecasting, a subtidal water level forecast system for the U.S. East Coast is under development which uses the two dimensional

barotropic Princeton Ocean Model with orthogonal curvilinear model grid (Fig.1). Grid resolution ranges from 5 to 32 km. The model is forced by a 48km EDAS analyzed wind field. An objective of this system is to forecast subtidal water levels along the East Coast and to provide water level forecasts as the open boundary condition for other regional or bay forecasting systems. With the ability to acquire real-time water gauge observations along the coast, it is now feasible to assimilate real time observed water levels into a numerical model, using the optimal control data assimilation technique in order to improve water level nowcasts and subsequent forecasts. From the sensitivity experiments of subtidal water level simulation, we found that the surface wind plays a predominant role in causing the subtidal water level variation in this area. Thus wind drag coefficients are chosen as the control variables in the data assimilation. The idea is based on the assumption that the forecast wind field is not accurate enough (and its resolution is also too coarse compared with the ocean model grid resolution), hence causing the water level misfits between observed and simulated water levels. For convenience we use a change in wind drag coefficients to represent (and correct for) systematic “errors” in the wind field. However, it is possible that there really could be errors in the wind drag coefficient, since its behavior as wind speed increases is still not well understood, especially at high wind speeds. A problem with the wind drag coefficient can also occur if the effect of atmospheric stability is not included in its formulation, in which case, changing air and water temperature could affect wind stress in an unaccounted for way. Thus, by assimilating the observed subtidal water level into a numerical model, it is possible to improve the wind field by adjusting the wind drag coefficients. In reality, surface wind drag coefficients are position-dependent parameters. In this paper, for the sake of simplification, the forward model is linearized, and the wind drag coefficients are assumed as constant or piecewise constants. Pseudo-observations generated by the numerical model with predefined wind drag coefficients are used in a twin identical experiment. The real observed subtidal water levels are obtained from total observed water level by a 30-hour low-pass Fourier filter.

## 2. Forward Numerical Model

### 2.1 Fully Two-dimensional POM Governing Equations

The governing equations of two dimensional POM are given as follows:

$$\frac{\partial \eta}{\partial t} + \frac{\partial UD}{\partial x} + \frac{\partial VD}{\partial y} = 0 \quad (1)$$

$$\frac{\partial UD}{\partial t} + \frac{\partial U^2 D}{\partial x} + \frac{\partial UVD}{\partial y} - F_x - fVD + gD \frac{\partial \eta}{\partial x} = \frac{1}{\rho} (\tau_{sx} - \tau_{bx}) \quad (2)$$

$$\frac{\partial VD}{\partial t} + \frac{\partial UVD}{\partial x} + \frac{\partial V^2 D}{\partial y} - F_y + fUD + gD \frac{\partial \eta}{\partial y} = \frac{1}{\rho} (\tau_{sy} - \tau_{by}) \quad (3)$$

where  $H$ ,  $\tau_s$  and  $\tau_b$  are water depth at rest, wind stress and bottom friction, and  $D=H+\eta$  total water depth,  $g$  the acceleration due to gravity,  $f$  the Coriolis parameter,  $\rho$  the water density. And the horizontal viscosity and diffusion terms  $F_x$  and  $F_y$  are defined as

$$F_x = \frac{\partial}{\partial x} \left[ H2A_M \frac{\partial U}{\partial x} \right] + \frac{\partial}{\partial y} \left[ HA_M \left( \frac{\partial U}{\partial y} + \frac{\partial V}{\partial x} \right) \right] \quad (4)$$

$$F_y = \frac{\partial}{\partial y} \left[ H2A_M \frac{\partial V}{\partial y} \right] + \frac{\partial}{\partial x} \left[ HA_M \left( \frac{\partial U}{\partial y} + \frac{\partial V}{\partial x} \right) \right] \quad (5)$$

where  $A_M$ , the vertically integrated horizontal eddy viscosity, is defined by the Smagorinsky formula

$$A_M = C\Delta x\Delta y \frac{1}{2} |\nabla V + \nabla V^T| \quad (6)$$

$C$ , a non-dimensional parameter, is set to be 0.2 in this study;  $\Delta x$  and  $\Delta y$  are the grid spacings in the  $x$  and  $y$  directions for each grid cell.

**Table 1. RMS Errors and Correlation Coefficients at 15 East Coast Locations**

Station	Mean_ob (cm)	Mean-M (cm)	RMS (cm)	RMS (demean) (Cm)	Correla	Correla (Demean)
Newl	5.13		-1.08	10	8	0.80
	0.91					
Brid	6.41		2.98	12	11	0.92
	0.91					
Montk	5.54		4.86	8	8	0.90
0.90						
Willets	7.53		4.65	15	15	0.91
0.91						
S H.	6.76		-2.51	11	9	0.79
0.87						
Atlantic	8.03		-0.45	13	9	0.77
0.89						
Lewes	7.54		-1.89	13	10	0.62
0.84						
Kipt.	7.83		-1.48	13	8	0.53
0.80						
Glou.	7.93		1.36	12	9	0.67
0.77						
CBBT	8.36		-1.37	14	10	0.55
0.79						
Duck	9.38		-0.59	14	10	0.52
0.68						
Cape	7.79		-1.01	12	8	0.28
0.54						
Spring	10.6		0.47	13	8	0.60
0.75						
Char.	11.5		0.24	14	8	0.55
0.73						
Mayport	13.2		2.27	16	11	0.71
0.75						

First, the fully nonlinear two-dimensional POM is used to evaluate numerical model subtidal water level simulation at 15 selected locations. The model simulates a period from Sep. 1 to Oct. 31, 1996. During this period, there were three hurricanes that occurred in Sep. 16-18, Oct. 7-9, and Oct. 16-20, respectively. The EDAS analyzed wind fields were used as the surface forcing. Wind stress is calculated using a formula developed by Large and Pond (1981). The results (Fig. 2) show that the variation trends of simulated water levels with time match that of observations fairly well at most locations most of the time. Mean values, correlation coefficient and Root Mean Square (RMS) of the differences between the observed and the simulated subtidal water levels are presented in Table 1. Note that there are mean value differences between the observed and the simulated subtidal water levels. The simulation mean value is lower than that of observation at most locations. The demeaned RMS errors range from 8 cm to 15 cm, the correlation coefficients between observed and simulated subtidal water levels vary from maximum 0.91 at Willets Point and New London to minimum 0.54 at Cape Hatteras. There are differences between the observed and simulated subtidal water levels even during the weak wind period. These differences are because the 2-D model forced by surface wind was run for only two months, so some low-frequency signals in the observed subtidal water levels which are caused by other factors were not represented in the simulated subtidal water levels. This includes steric effects on water level due to water temperature change, which are not included in the model, as well as Gulf Stream effects on the southern stations.

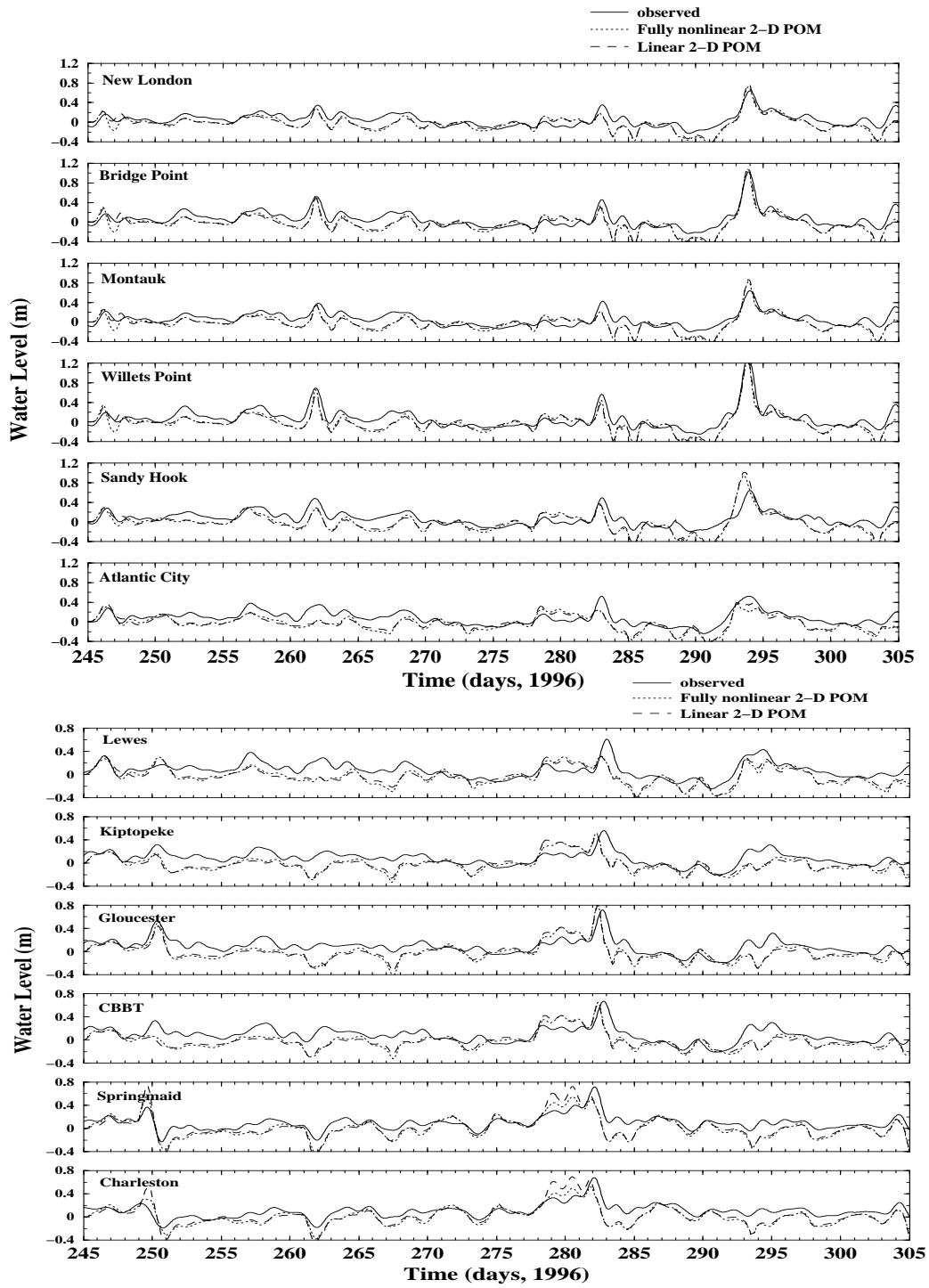


Fig. 2. Comparison of observed and simulated subtidal water levels without data assimilation at NOS tide gauge locations.

## 2.2 Linearized Governing Equations

To simplify the adjoint model development, the fully nonlinear two-dimensional POM is linearized by: (1) neglecting the variation of water level surface elevation  $\eta$  relative to water depth ( $D=H$ ), which is reasonable for the depths over most of model regime; (2) neglecting the horizontal advection and diffusion terms ( $F_x$  and  $F_y$ ); (3) linearizing the bottom friction terms (which is also reasonable for the depths over most of the regime) with a constant bottom friction coefficient,  $C_b = 1.0 \times 10^{-3}$ . Thus, the linearized 2-D POM governing equations are as follows,

$$\frac{\partial h}{\partial t} + \frac{\partial HU}{\partial x} + \frac{\partial HV}{\partial y} = 0 \quad (7)$$

$$\frac{\partial HU}{\partial t} - fHV + gH \frac{\partial h}{\partial x} + C_d |U_w| \cdot U_w - C_b U = 0 \quad (8)$$

$$\frac{\partial HV}{\partial t} + fHU + gH \frac{\partial h}{\partial y} + C_d |U_w| \cdot V_w - C_b V = 0 \quad (9)$$

The model is integrated from rest, and radiational open boundary conditions are used on the southern boundary. The results of the linearized POM (Fig. 2) demonstrate that, for subtidal water level simulation, the linearized 2-D POM gives results similar to those of the fully nonlinear 2-D POM. Therefore, it is reasonable to implement the linearized 2-D POM to simulate subtidal water levels for this coastal ocean area.

## 3. Adjoint Equations of Linearized 2-D POM

The adjoint method is increasingly being implemented in data assimilation, model tuning, and model sensitivity analysis. It provides an efficient method for calculating the gradients of cost function with respect to control variables (especially in the case of large number of control variables). However, the adjoint equations depend on the forward equations, and derivation of adjoint equations is complicated. Zhu et al. (1997a) simply described the construction of an adjoint model for the 2-D barotropic model of Institute of Atmospheric Physics of China (IAP) and applied it to estimate the open boundary conditions of a tidal model (Zhu et al., 1997b). Ralf and Kaminski (1996) and Ralf (1997) proposed a helpful and basic textbook on how to construct adjoint code from forward model code using a tangent linear compiler (TLC). However, in this particular application, it is difficult to determine what the formula is to calculate the gradient from the adjoint variables. In some occasions, TLC may even generate redundant statements in the adjoint code. Here, as an example for the linearized 2-D POM with well-posed initial and open boundary conditions, the procedure for deriving adjoint equations is presented in continuous notation.

In oceanic numerical modeling we are often confronted with some unknown or

undetermined parameters, e.g., initial conditions, open boundary conditions, friction coefficients, wind drag coefficients, etc. In this study, we are concerned with nontidal elevation data assimilation. Since wind stresses play the most important role in nontidal elevation simulation, the surface wind drag coefficient  $C_d$  is chosen as the control variable.

The basic procedure in the variational adjoint method consists of minimizing a cost function that represents the misfits between observed data and model output. This minimization is performed subject to the strong constraints of satisfying the governing equations. The constraint minimization involves Lagrange multipliers and leads to additional equations (known as adjoint equations) from which Lagrange multipliers are determined. The model state variables and Lagrange multipliers are used to compute the cost function and its gradient from which the cost function is minimized to obtain the optimal control variables.

In this variational problem the cost function is defined as,

$$J = \frac{1}{2} \iiint_{xyt} W(h - h_o)^2 dx dy dt \quad (10)$$

where  $h_o$  and  $h$  are observed and simulated elevations and  $W$  is the weighting factor. The variational problem is to minimize cost function  $J$  subject to equations (7)-(9). Introducing Lagrange multipliers  $\lambda_h, \lambda_u, \lambda_v$  for the constraint governing equations (7), (8), (9) (Lawson et al, 1995), the first variation of the cost function  $J$  can be written as

$$\begin{aligned} \delta J = & \iiint_{xyt} \left[ (h - h_o) + \lambda_h \delta \left( \frac{\partial h}{\partial t} + \frac{\partial HU}{\partial x} + \frac{\partial HV}{\partial y} \right) \right. \\ & + \lambda_u \delta \left( \frac{\partial HU}{\partial t} - fHV + gH \frac{\partial h}{\partial x} + C_d |U_w| \cdot U_w - C_b U \right) \\ & \left. + \lambda_v \delta \left( \frac{\partial HV}{\partial t} + fHU + gH \frac{\partial h}{\partial y} + C_d |U_w| \cdot V_w - C_b V \right) \right] dx dy dt \end{aligned} \quad (11)$$

The corresponding adjoint variables are defined as follows:  $\lambda_h$  is the adjoint variable of  $h$ ,  $\lambda_u$  is the adjoint variable of  $U$ , and  $\lambda_v$  is the adjoint variable of  $V$ , respectively.

Considering the specific case defined above, using wind drag coefficients as the only control variables, Eq. (11) can be rewritten as, after applying the chain rule and integrating by parts,

$$\begin{aligned}
\delta J = & \iiint_{xyt} \left[ (h - h_o) - \frac{\partial \lambda_h}{\partial t} - g \frac{\partial H \lambda_u}{\partial x} - g \frac{\partial H \lambda_v}{\partial y} \right] \delta h \, dx dy dt \\
& + \iiint_{xyt} \left( -H \frac{\partial \lambda_h}{\partial x} - H \frac{\partial \lambda_u}{\partial t} - C_b \lambda_u + f H \lambda_v \right) \delta U \, dx dy dt \\
& + \iiint_{xyt} \left( -H \frac{\partial \lambda_h}{\partial y} - H \frac{\partial \lambda_v}{\partial t} - C_b \lambda_v - f H \lambda_u \right) \delta V \, dx dy dt \\
& + \iiint_{xyt} (\lambda_u |U_w| U_w + \lambda_v |U_w| V_w) \delta C_d \, dx dy dt \\
& + \iint_{xy} (\lambda_h \delta h + H \lambda_u \delta U + H \lambda_v \delta V) \, dx dy \Big|_0^T \\
& + \iint_{xt} (g H \lambda_v \delta h + H \lambda_h \delta V) \, dx dt \Big|_0^Y \\
& + \iint_{yt} (g H \lambda_u \delta h + H \lambda_h \delta U) \, dy dt \Big|_0^X
\end{aligned} \tag{12}$$

Since the initial conditions and boundary conditions are well-posed for this specific case described earlier, we have

$$\begin{aligned}
\delta h \Big|_{t=0} = \delta U \Big|_{t=0} = \delta V \Big|_{t=0} = 0 \\
\delta h \Big|_{x=0}^{x=X} = \delta U \Big|_{x=0}^{x=X} = \delta V \Big|_{x=0}^{x=X} = 0 \\
\delta h \Big|_{y=0}^{y=Y} = \delta U \Big|_{y=0}^{y=Y} = \delta V \Big|_{y=0}^{y=Y} = 0
\end{aligned}$$

Therefore, the last three terms of (12) are zero if the initial values (t=T) of  $\lambda_u$ ,  $\lambda_v$ , and  $\lambda_h$  are forced to be zero. By forcing the coefficients of the non-control variables ( $\delta h$ ,  $\delta U$ ,  $\delta V$ ) to zero, we obtain adjoint equations as follows,

$$H \frac{\partial \lambda_u}{\partial t} - f H \lambda_v + H \frac{\partial \lambda_h}{\partial x} + C_b \lambda_u = 0 \tag{13}$$

$$H \frac{\partial \lambda_v}{\partial t} + f H \lambda_u + H \frac{\partial \lambda_h}{\partial y} + C_b \lambda_v = 0 \tag{14}$$

$$\frac{\partial \lambda_h}{\partial t} + g \left( \frac{\partial H \lambda_u}{\partial x} + \frac{\partial H \lambda_v}{\partial y} \right) = h - h_o \tag{15}$$

and the function increment becomes

$$\delta J = \iiint_{xyt} (\lambda_u |U_w| U_w + \lambda_v |U_w| V_w) \delta C_d \, dx dy dt \tag{16}$$

The above process showed that cost function minimization has resulted in new equations (13)-(15) which are called adjoint equations. And the adjoint variables are calculated by integrating the adjoint equations. The gradient of the cost function with respect to the control variable, wind drag coefficient  $C_d$ , can be computed by

$$G = \iiint_{xyt} (\lambda_u |U_w| U_w + \lambda_v |U_w| V_w) \, dx dy dt \tag{17}$$

It is shown from (17) that, if  $C_d$  varies spatially and temporally, the gradients of cost

function with respect to  $C_d$  can be computed by integrating the adjoint model once regardless of the number of control variables.

By comparison with 2-D forward POM equations, it is seen that the adjoint equations (13)- (15) are similar to their original model equations (7)-(9). The differences between forward and adjoint equations are: no wind stress forcing terms are included in adjoint equations because the wind drag coefficient is defined as control variable; the data misfit ( $h-h_o$ ) is added to adjoint equation as a forcing term; the friction terms in the adjoint equations and the corresponding governing equations have opposite signs. This implies that the adjoint equations have to be integrated backwards in time starting from zero values at the final time step.

An iterative scheme for a 24-hour data assimilation is given in Fig.3.

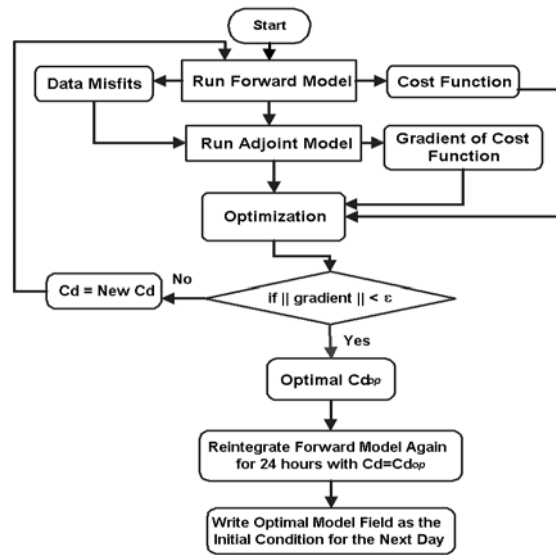


Fig. 3. Flow Chart for a 24-Hour Water Level Data Assimilation Run

#### 4. Identical Twin Experiments

In order to check the performance of adjoint optimal data assimilation technique, identical twin experiments are usually considered. In twin experiments, the pseudo-observed water level data are generated by the numerical model. This is the best situation for data assimilation since the pseudo-observational data contain the same dynamics as the numerical model and are not contaminated by any error. In this study, the pseudo-subtidal water levels are generated by integrating the model with a constant or piecewise constant predefined wind drag coefficient over the entire

domain and hourly subsampled at 15 selected locations. With a known initial condition from the model spin-up and the radiation formula implemented on southern open boundary, three cases are devised in the one- and 30- day data assimilation simulations. These are:

- Case 1: pseudo-observations contain no errors,
- Case 2: pseudo-observations at all locations are contaminated with a random white noise which has zero mean value and a standard deviation 0.029 m,
- Case 3: same as Case 2 except the white noise standard deviation is doubled to 0.058 m.

#### 4.1 One-day Data Assimilation

One-day pseudo-observations at 15 selected locations are used to recover the wind drag coefficient in this one-day data assimilation experiment (for convenience, the value of  $C_d$  appeared in this paper, including figures and tables, is multiplied by  $10^3$ ). The forward model is integrated from rest with a true  $C_d$  as 10.0. In the data assimilation procedure, the first guess  $C_d$  is 20.0. The variation of the optimal  $C_d$ , the gradient of the cost function, and the cost function are plotted as a function of the iteration number in Fig. 4 and the final values are listed in Table 2. For Case 1, the optimal  $C_d$  converges to the true value after three iterations and the corresponding gradient and cost function are less than  $10^{-8}$ . For Cases 2 and 3, the optimal  $C_d$ s tend close to (but not exactly converge to) their true solutions after four iterations and the cost functions are much greater than that of Case 1. By comparison of the data misfits (the difference between the model results and the observations) and the noise added the observations, it is found that the curves of the misfits and noise for each station are very similar. This indicates that the value of the cost function is primarily contributed by the noise. The noise results in the optimization line search routine failing to find a better converging direction for optimizing procedure. Thus the optimization procedure could not recover the true  $C_d$ . This experiment indicates that observation errors can affect the optimal results.

#### 4.2 30-day Continuous Data Assimilation

**Table 2. Final optimal  $C_d$ , gradient and cost function**

	Optimal $C_d$	Gradient	Cost function
Case 1	9.99998	$-3.197 \times 10^{-8}$	$7.0 \times 10^{-10}$
Case 2	10.085	$2.07 \times 10^{-6}$	0.138
Case 3	10.170	$-4.88 \times 10^{-6}$	0.553

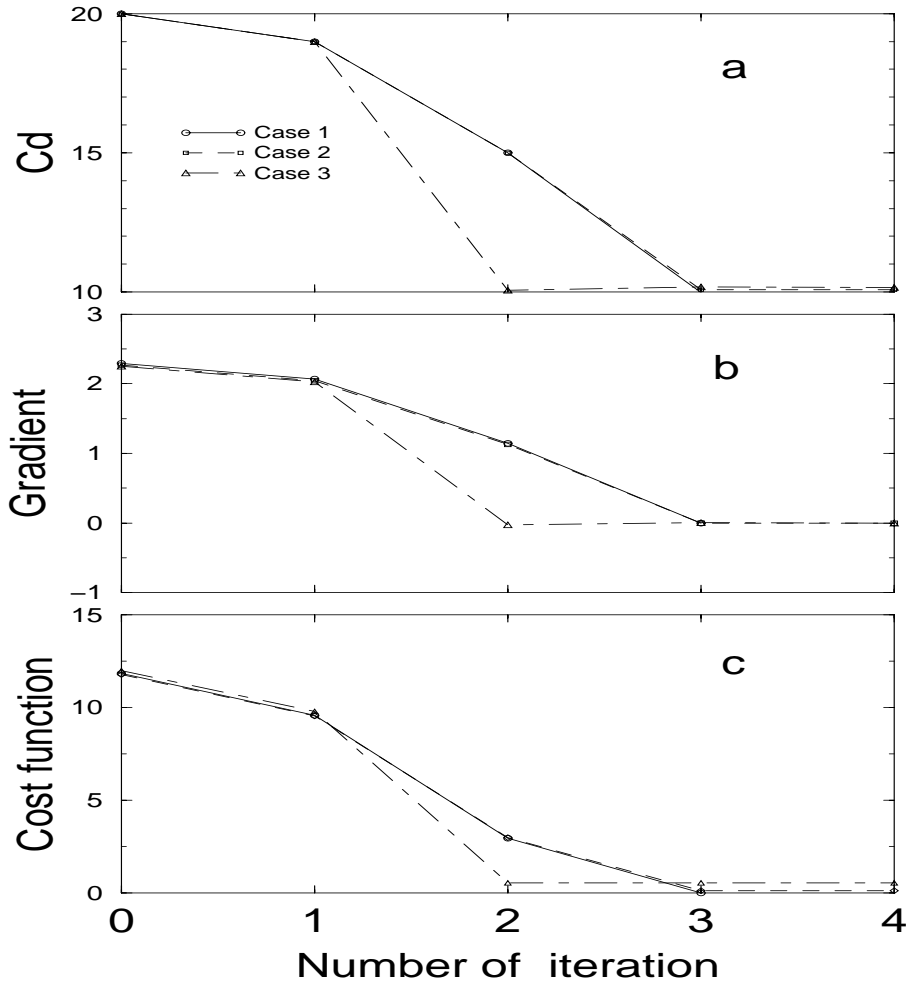


Fig.4. The variation of parameters with number of iteration in the one-day identical twin data assimilation: (a) the optimal  $C_d$ ; (b) the gradient of the cost function; and (c) the cost function.

#### 4.2 30-day Continuous Data Assimilation

The three cases described above are repeated in a 30-day continuous data assimilation. The true wind drag coefficient  $C_d$  is set as a function of time, but constant within each day. The forward model starts from rest and creates a restart file at the end of each day as the initial condition for next day's data assimilation. The first guess  $C_d$  of the first day is 20.0 and the optimal  $C_d$  of the previous day is used as the first guess  $C_d$  for the next day's data assimilation. The time series of the final optimal  $C_d$ , the gradient of the cost function, and the cost function are plotted in Fig. 5. The maximum of difference between true and final optimal  $C_d$ , the maximum of

gradients and the maximum of the cost functions from each case are presented in Table 3. For Case 1 with no observational error, the data assimilation procedure recovers the optimal  $C_d$  to its true value. The cost function and its gradient are less than  $10^{-9}$  and  $10^{-7}$ , respectively.

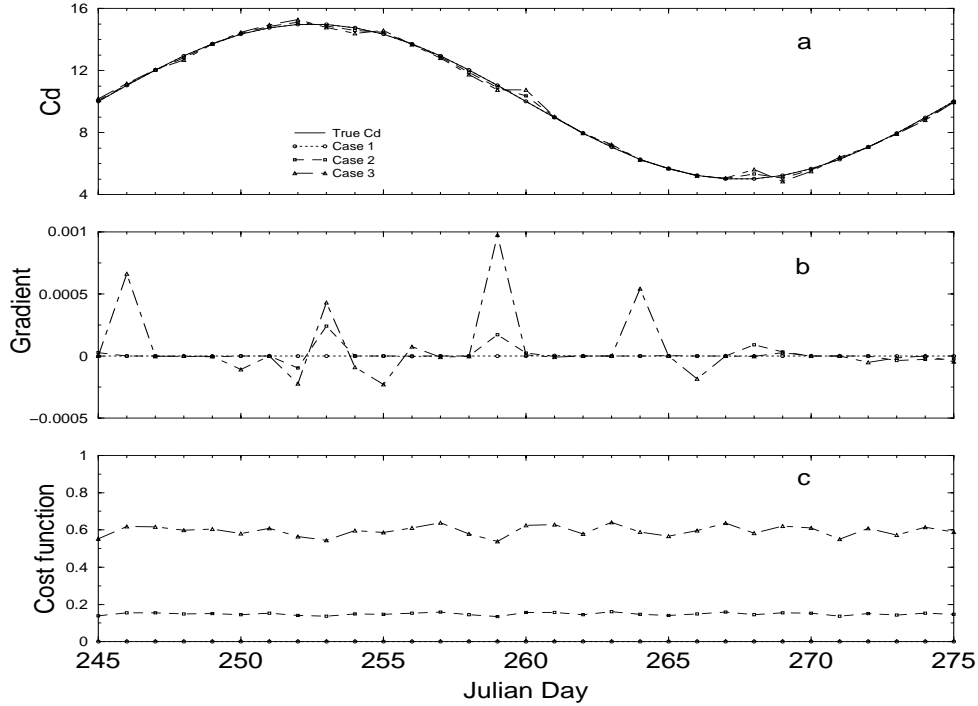


Fig.5 Time series of parameters in the 30-day identical twin data assimilation: (a) the optimal  $C_d$ ; (b) the final gradient of the cost function; and (c) the final cost function.

For Case 2, the recovered optimal  $C_d$  is also close to its true value. However, the cost function is much greater than that of Case 1. As described in the one-day simulation, the value of the cost function is primarily contributed by the random noise added to the pseudo-observations. By adding the white noise to the pseudo-observations, the forward model can not dynamically simulate the random noise so that the final optimal  $C_d$  can not coverage to the true  $C_d$ .

For Case 3, by doubling the standard deviation of random noise, most of the optimal  $C_d$ s are also close to the true values. However, the differences between optimal  $C_d$ s and true  $C_d$ s are much greater than that of Cases 1 and 2. The cost function and its gradient are the greatest among three cases.

For the continuous data assimilation cases, the restart field is generated by the previous day forward model integration. If there is a difference between the optimal

$C_d$  and its true  $C_d$  in the previous day, the restart field with the optimal  $C_d$  will be different from true initial field of this day. Then the optimal  $C_d$  may not converge to its true value in this day data assimilation.

**Table 3. The Maximum of difference between the true and the final optimal  $C_d$ , the maximum of cost Functions and maximum of Gradients**

	$Max\ Cd_{optimal} - Cd_{true}\ $	$Max\ Gradient\ $	$Max\ Cost Function\ $
Case 1	$2.0 \times 10^{-5}$	$3.16 \times 10^{-8}$	$8.5 \times 10^{-10}$
Case 2	0.37	$3.4 \times 10^{-5}$	0.16
Case 3	0.74	$9.77 \times 10^{-4}$	0.64

### 4.3 One-day Identical Twin Experiment with Eight Control Variables

The wind drag coefficient should be time and position dependent. This is not simply because we use the Large-Pond formulation for  $C_d$ , in which  $C_d$  depends on wind speed, which itself is time and position dependent. In finding optimal  $C_d$ s as part of a data assimilation scheme, we are allowing the “improvement” in  $C_d$  to represent (and correct for) a systematic error in the wind field, which varies in space and time.

In order to test the performance of the adjoint data assimilation system for the multi-control variables case, the experiment with eight piecewise constant control variables is devised and performed. In this experiment, the entire domain is divided into eight pieces, and the wind drag coefficient in each piece is constant and used as one control variable (see Fig.1). The true solution of  $C_d$  is expressed as

$$C_{dm} = 10.0 + 5.0 \sin\left[\frac{2\pi}{30.0}(m-1)\right] \quad m=1,2,\dots,8 \quad (18)$$

here  $m$  denotes the index of control variable in each subregion. The initial guesses for all of  $C_d$  are set to be 20.0. The result of this experiment shows that, in the first several iterations, most of the optimal  $C_d$  components (Fig.6) converge towards their true solutions very fast. The optimal  $C_d$  values for all of the eight components are very close to their true values after about 10 iterations. The maximum difference between the true solution and the final optimal  $C_d$  for all eight control variables is  $1.5 \times 10^{-4}$ , which appeared at the eighth control variable component. The cost function and the norm of the gradient (Fig.7) drop rapidly in the first three iterations. The convergence criterion  $\|G\| < 10^{-7}$  is satisfied after 30 iterations, and the corresponding values of the cost function and the norm of the gradient are  $1.4 \times 10^{-11}$  and  $3.2 \times 10^{-8}$  respectively.

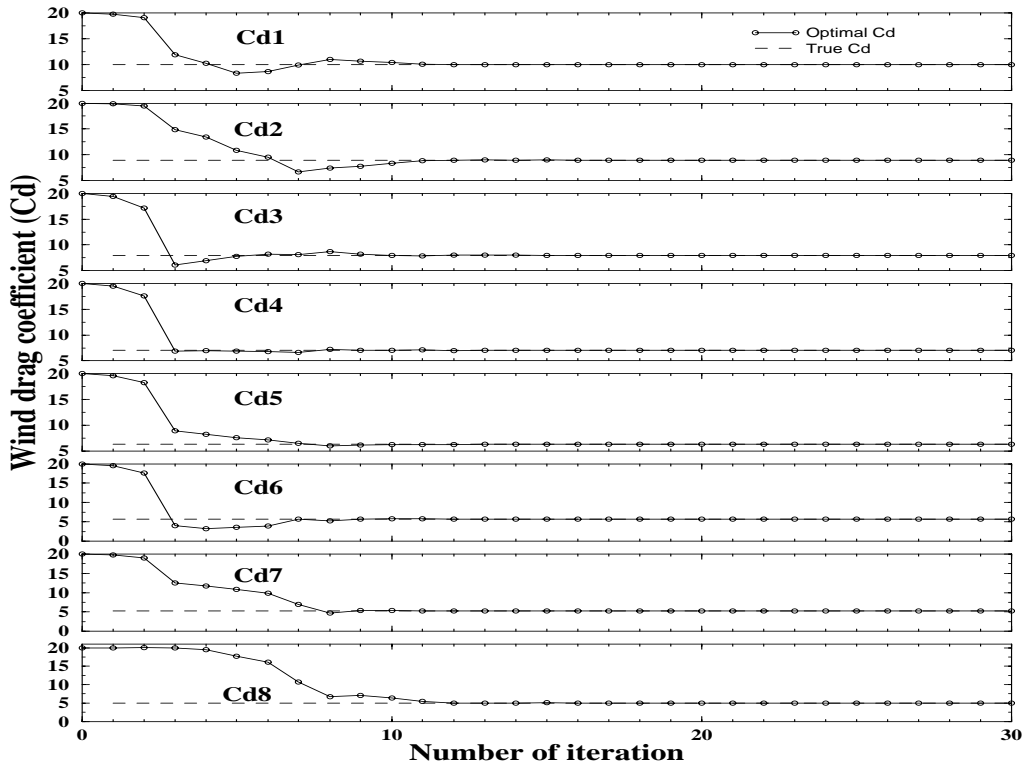


Fig.6. Variation of the optimal  $C_d$  components with the number of iterations for one day identical experiment with eight control variables.

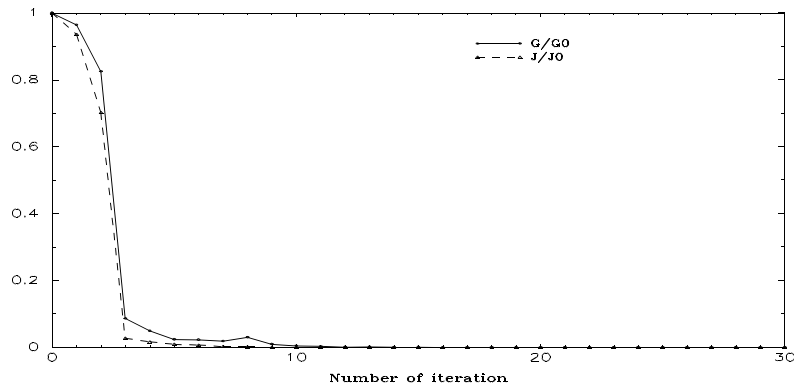


Fig.7. Variation of the norm of the gradient  $\frac{\|G\|}{\|G_0\|}$  and the cost function  $J/J_0$  with the number of iterations one day identical experiment with eight control variables. Where  $J_0$  and  $\|G_0\|$  are initial values of the cost function and its gradient.

In order to examine the effects of the initial guesses of  $C_d$  on the optimization procedure, different initial guesses are tested. The results show that no matter how far the first guesses are away from their true solutions, the cost function and the norm of the gradient drop rapidly in the initial several iterations, and the optimal  $C_d$ s are very close to their true solutions after about ten iterations. After that, the optimization procedure adjusts the optimal  $C_d$  slowly, and all of the eight optimal  $C_d$  components gradually converge to their true solutions.

## 5. Summary

From the experiments described in previous sections, we conclude that:

- a. The linearized 2-D POM simulates the subtidal water level fairly well for this coastal ocean. The demeaned RMS errors and correlation coefficients are 9 cm and 0.87 at Sandy Hook and 10 cm and 0.79 at CBBT, respectively.
- b. For perfect pseudo-observations, the adjoint data assimilation system can exactly recover the true wind drag coefficient for both of the one and eight control variable experiments.
- c. Since water level observational errors have an impact on the wind drag coefficient recovery, the optimal  $C_d$  may not converge to its true value if the errors are significant.
- d. The errors in initial field play a very important role in recovering the wind drag coefficient.

## Acknowledgments

We would like to thank Dr. Yuanfu Xie of NOAA's Forecast System Laboratory for his assistance and great discussion in the construction of the adjoint model.

## References

- Aikman, F A., III, G. L. Mellor, D. Sheinin, P. Chen, L. Breaker, K. Bosley and D. B. Rao, 1996. "Towards an operational nowcast/forecast system for the U.S. East Coast". *Modern Approaches to Data Assimilation in Ocean Modeling*, 61, P. Malanotte-Rizzoli, Ed., Elsevier Publishers, 347-376.
- Blumberg, A. F. and G. L. Mellor, 1987. "A description of a three-dimensional coastal ocean circulation model." *Three Dimensional Coastal Ocean Models*. N. S. Heaper, Amer. Geophys. Union, 1-16.
- Chu, P., C. Fan, and L. L. Ehret, 1997. "Determination of open boundary conditions with optimization method. *J. Atmos. And Oceanic. Tech.*, Vol. 14, 723-734.
- Das, S. K. and R. W. Lardner, 1991. "On the estimation of parameters of hydraulic models by assimilation of periodic tidal data." *J. Geophys. Res.*, Vol.96, C8, 15187-15196.

- Ezer, T. and G. L. Mellor, 1997. "Data assimilation experiments in the Gulf Stream Region: how useful are satellite-derived surface data for nowcasting the subsurface fields". *J. Atmos. Oceanic Tech.*, 14, 1379-1391.
- Large, W. G., and S. Pond, 1981. "Open ocean momentum flux measurements in moderate to strong winds." *J. Phys. Oceanogr.*, Vol.11, 324-336.
- Lawson, L. M, Y. h. Spitz, E. E. Hofmann, and R. B. Long. (1995). "A data assimilation technique applied to a predator-prey model. *Bulletin of Mathematical Biology*, 1995, 57, 593-617.
- Liu, D. and J. Nocedal, 1989. "On the limited memory BFGS method for large scale optimization." *Mathematical Programming*, B 45, 503-528.
- Mellor, G. L., 1991. "User's guide for a three dimensional, primitive equation, numerical ocean model." Princeton University.
- Mellor, G. L. and T. Ezer, 1991. "A Gulf Stream model and an altimetry assimilation scheme". *J. Geophys. Res.*, 96, 8779-8795.
- Panchang, V. G. and J. J. O'Brien, 1989. "On the determination of hydraulic model parameters using the adjoint state formulation." *Modeling Marine Systems*. Edited by A. M. Davies, CRC Press, Boca Racon, 6-18.
- Ralf, G. and T. Kaminski, 1996. "Recipes for adjoint code construction." Technical Report 212, 1996, p35. Max-Planck-Institut fur Meteorologie.
- Ralf, G., 1997. "Tangent Linear and Adjoint Model Compiler. Users Manual, MIT, 53p.
- Sasaki, Y., 1970a. "Some basic formalisms in numerical variational analysis." *Monthly Weather Review*, Vol.98, No.12, 875-883.
- Sasaki, Y., 1970b. "Numerical variational analysis formulated under the constraints as determined by longwave equations and a low-pass filter." Vol.98, No.12, 884-899.
- Schwab, D. J., 1982. "An inverse method for determining wind stress from water level fluctuations." *Dyn. of Atmos. And Oceans.*, 6, 251-278.
- Yu, L. and J. J. O'Brien, 1991. "Variational estimation of the wind stress drag coefficient and the oceanic eddy viscosity profile." *J. Phys. Oceanogr.*, Vol. 21, 709-719.
- Zhu, J., Q. C. Zeng, D. J. Guo and C. Liu, 1997a. "The Construction of adjoint model of IAP barotropic model and its second-order adjoint model." *Science in China*. 27(3), 277-283. (In Chinese)
- Zhu, J., Q. C. Zeng, D. J. Guo and C. Liu, 1997b. "Estimation of the open boundary conditions of tidal model from coastal tidal observations by the adjoint method." *Science in China*, 1997, 27(5), 462-468. (In Chinese)

key words

Subtidal Water Level, Two-Dimensional POM, Adjoint Variational Data Assimilation,  
Parameter Estimation, Cost Function, Wind Drag Coefficient, Twin Experiment.